

Interactive comment on “Groundwater flow and storage within an alpine meadow-talus complex” by A. F. McClymont et al.

A. F. McClymont et al.

alastairmcclymont@gmail.com

Received and published: 1 May 2010

Following are our responses to the points raised by Reviewer 1. Pages, figure and line numbers are for the original manuscript. Some new figures have been uploaded. Revised Figure captions are below.

REVIEWER 1 (Anonymous)

1. Figure 1. We have experimented using gray levels to display topography in this figure but have found that the best way to show both topography and physiographic features like lakes and the glaciers is to use contours.

2. Figure 2b. We agree with both reviewer's comments on Figure 2 and have separated Figure 2a and Figures 2b-c into two new figures (now Figures 2 and 3)

C714

3. Figure 2b. We have enlarged this figure (now Figure 3a) and have made the geophysics profile lines thicker.

4. Figure 6. This is a good point and we have modified this figure (now Figure 9) to show the same color scales for Figure 9a and b.

5. Page 1550, line 22. We have revised this sentence to “As the meadow vegetation was growing during the snow-free season of July 1 - September 30...”.

6. Figure 7c. We agree with the reviewer and have removed these two points, which are not integral to our analysis.

7. Page 1552, line 9. We have revised this sentence to “ a conceptual diagram of the talus-meadow complex”

Revised Figure Captions

Figure 1. Topographic map of the Opabin watershed showing Opabin Creek (gray solid line), major lakes (gray bodies), a glacier (stippled), and the automatic weather station (AWS). Black square indicates the location of the hydrological and geophysical surveys on the talus-meadow complex shown in Figures 2 and 3. Contour interval is 50 m. The insert shows the site location in North America.

Figure 2. Three-dimensional photo-draped digital elevation model of the talus-meadow complex (outlined by dashed line). White line - small stream that flows intermittently across the meadow and drains into a neighboring gully. No vertical exaggeration. Coordinates are in UTM grid.

Figure 3. (a) Contour map of the same region shown in Figure 2 with location of the five GPR profiles (red lines), centers of five common-midpoint (CMP) GPR profiles (red circles), four ERT profiles (green lines), and the shot and receiver array of the seismic refraction profile (dark blue line). Yellow body shows the area of the alpine meadow and gray body the area of the talus cones. Also shown are the locations of four piezometers (black circles), the monitoring weir (triangle), and the excavated

C715

soil pit (square). Blue dotted line - course of the small stream. Contour elevations are in meters. (b) Photo of the talus-meadow complex taken from the top of profile GPR1/ERT1 and looking to the southwest. Also shown are the locations of piezometers P1-P4 and profile GPR2/ERT2.

Figure 4. Processed GPR cross-sections from profiles (a) GPR1 and (b) GPR2. Profile locations are shown in Figure 3a. Block arrows show where the two lines intersect. Three zones with different surface characteristics are demarcated: meadow, unvegetated talus and vegetated talus. The dots in (b) mark the projected locations of the center of the CMP1 GPR profile, piezometer P1 and the cluster of piezometers P2-P4 onto profile GPR2. AW and GW in (b) indicate the airwave and groundwave phases, respectively.

Figure 5. (a) GPR data from CMP1, which was recorded using 50 MHz antennas (location shown in Figure 3a). Solid line shows the linear moveout of the picked airwave phase (V_a); dashed lines show the linear moveout of a slow groundwave phase attributed to a thin soil layer (V_{g1}), and the normal moveout of a subsurface reflection (V_{r1}); dotted line shows the linear moveout of a second fast groundwave phase attributed to a substrate of bedrock underlying the meadow (V_{g2}). (b) Corresponding semblance plot for which warmer colours represent higher values. Circle defines the normal moveout velocity calculated for picked reflection V_{r1} shown in (a).

Figure 6. As for Figure 4, but with the corresponding inverted electrical resistivity tomograms ERT1 and ERT 2 overlain onto the GPR cross-sections. ERT model cells with DOI values >0.2 are not plotted (see text for explanation).

Figure 7. Example shot gather recorded from shot point 5 (SP5), which was located on a talus deposit (the shot point location is shown on the seismic tomogram in Figure 8). Circles are observed first-break picks and squares are calculated travel-times from the inverted velocity model.

Figure 8. (a) Inverted p-wave velocity tomogram for the seismic refraction profile (lo-

C716

tion shown in Figure 3a). Shot-receiver raypaths calculated for the model are plotted as black lines. Shot gather data from shot point SP5 are shown in Figure 7. (b) The same p-wave velocity tomogram as shown in (a) but plotted as a transparent overlay onto the corresponding cross-section for profile GPR1. Regions of the model that are not traversed by the raypaths shown in (a) are not plotted.

Figure 9. Contoured maps of (a) meadow topography from 2-m LIDAR DEM, (b) subsurface bedrock topography produced by interpolating bedrock picks made on ERT and GPR profiles, and (c) depth to bedrock produced by differencing (a) and (b). Dotted line – surface stream channel; circles – piezometers P1-P4 and the center of the CMP1 GPR profile; triangle – monitoring weir; square – excavated soil pit.

Figure 10. Hydrological data for June-September, 2008. (a) Daily precipitation. (b) Elevation (above mean sea level) of the water level in piezometer P4. Dashed line indicates the ground surface at this location. (c) Discharge measured at the weir. See Figures 3a and 9 for the location of P4 and the weir.

Figure 11. Schematic diagram showing the internal structure and groundwater and surface water flow pathways in the talus-meadow complex.

Interactive comment on Hydrol. Earth Syst. Sci. Discuss., 7, 1535, 2010.

Figure 2

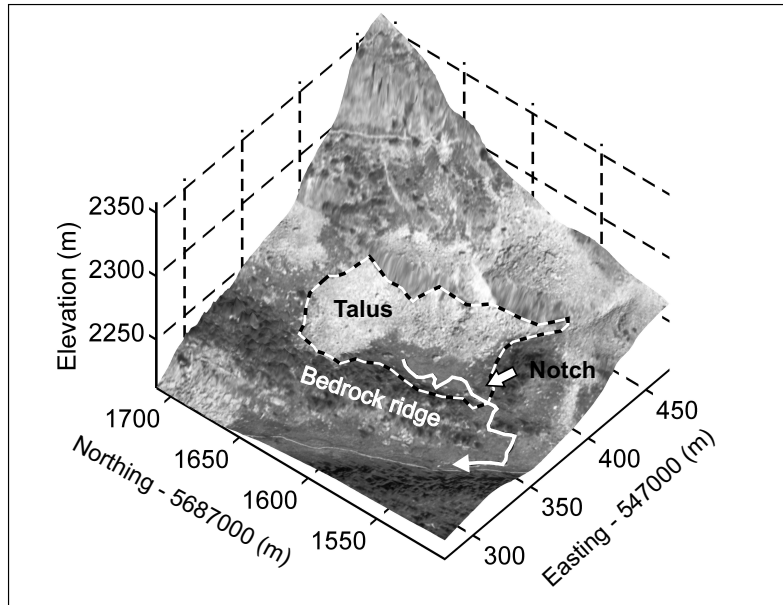


Fig. 1. Figure 2

C718

Figure 3

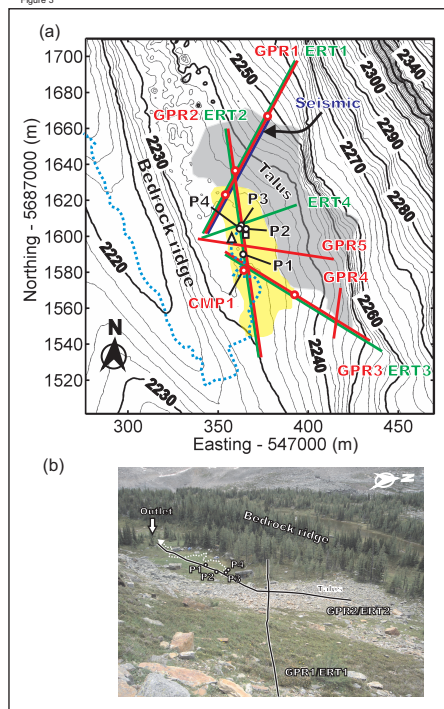


Fig. 2. Figure 3

C719

Figure 9

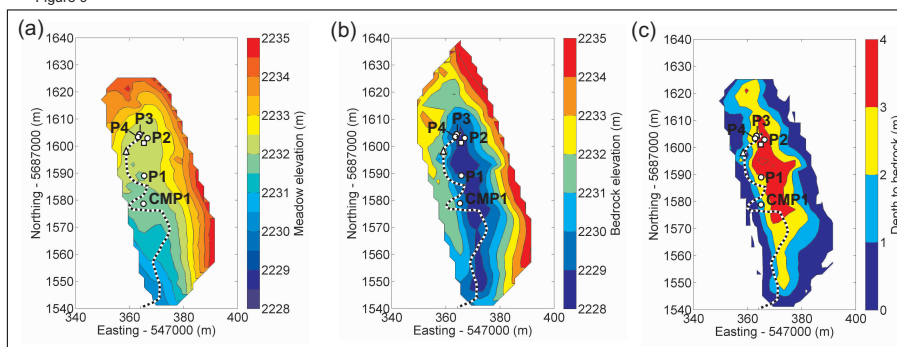


Fig. 3. Figure 9

C720

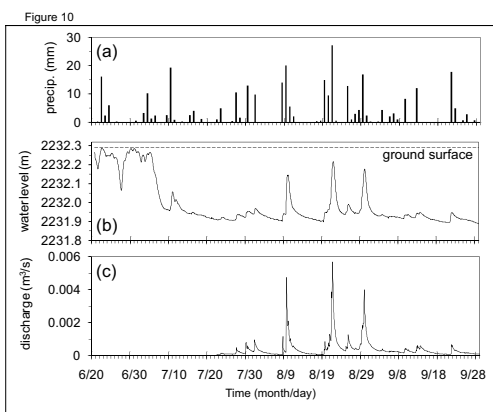


Fig. 4. Figure 10

C721